

Article

# Improvement in the Lifetime of Planar Organic Photovoltaic Cells through the Introduction of MoO<sub>3</sub> into Their Cathode Buffer Layers

Linda Cattin <sup>1</sup>, Mustapha Morsli <sup>2</sup> and Jean Christian Bern ède <sup>3,\*</sup>

- Institut des Mat ériaux Jean Rouxel (IMN), UMR 6502, Universit éde Nantes, CNRS,
  2 rue de la Houssini ère, BP 32229, F-44322 Nantes cedex 3, France;
  E-Mail: linda.cattin-guenadez@univ-nantes.fr
- L'UNAM, Université de Nantes, Faculté des Sciences et des Techniques, 2 rue de la Houssinière, BP 92208, F-44000 Nantes, France; E-Mail: Saber.Morsli@univ-nantes.fr
- <sup>3</sup> L'UNAM, Université de Nantes, MOLTECH-Anjou, CNRS, UMR 6200, 2 rue de la Houssini ère, BP 92208, F-44000 Nantes, France
- \* Author to whom correspondence should be addressed; E-Mail: jean-christian.bernede@univ-nantes.fr; Tel.: +33-251-125-530.

Received: 11 January 2014; in revised form: 14 February 2014 / Accepted: 24 February 2014 / Published: 6 March 2014

Abstract: Recently, MoO<sub>3</sub>, which is typically used as an anode buffer layer in organic photovoltaic cells (OPVCs), has also been used as a cathode buffer layer (CBL). Here, we check its efficiency as a CBL using a planar heterojunction based on the CuPc/C<sub>60</sub> couple. The CBL is a bi-layer tris-(8-hydroxyquinoline) aluminum (Alq<sub>3</sub>)/MoO<sub>3</sub>. We show that the OPVC with MoO<sub>3</sub> in its CBL almost immediately exhibits lower efficiency than those using Alq<sub>3</sub> alone. Nevertheless, the OPVCs increase their efficiency during the first five to six days of air exposure. We explain this evolution of the efficiency of the OPVCs over time through the variation in the MoO<sub>3</sub> work function due to air contamination. By comparison to a classical OPVC using a CBL containing only Alq<sub>3</sub>, if it is found that the initial efficiency of the latter is higher, this result is no longer the same after one week of exposure to ambient air. Indeed, this result is due to the fact that the lifetime of the cells is significantly increased by the presence of MoO<sub>3</sub> in the CBL.

**Keywords:** planar organic photovoltaic cells; cathode buffer layer; molybdenum oxide; lifetime; air contamination; work function

## 1. Introduction

Recent studies show that if current progress is continued, organic photovoltaic cells (OPVCs) will have a unique advantage for large scale power generation [1]. The method often used to increase the efficiency of OPVCs consists of the introduction of buffer layers between the electrodes and the organic films [2,3]. These buffer layers must improve the collection efficiency of one type of carrier and must be selective by opposing the passage of carriers of the opposite sign. Moreover, these buffer layers improve the band matching between the electrodes and the organic materials. In classical OPVCs, the anode buffer layer (ABL) can also smooth the surface of the ITO electrode, while the cathode buffer layer (CBL), often called the exciton blocking layer, protects the electron acceptor from metal diffusion during thermal evaporation of the cathode. However, the lifetime of OPVCs is far from satisfactory. The lifetime is mainly dependent on the environment. Important environmental parameters that influence the lifetime of organic solar cells are the diffusion of oxygen and water into the active layers of the cells through the upper electrode [4–6]. A possible solution to the problem of contaminant diffusion into the active organic layers could be the use of barrier layers with low oxygen and water permeability. The use of buffer layers could contribute to this solution. MoO<sub>3</sub> is a very efficient ABL [7,8]. However, there is some controversy about its band structure. It is now well accepted that its band gap is approximately 3.1 eV and that it is an *n*-type material, yet the values of its ionization potential (IP), its electronic affinity  $(\chi)$ , and its Fermi level (Wf) are still under discussion. These values measured in situ by ultraviolet photoelectron spectroscopy (UPS) after deposition in ultra-high vacuum are IP = 9.7 eV,  $\chi$  = 6.7 eV and Wf = 6.9 eV. After air contamination, these values decrease significantly. It is well known that after five minutes or more of air exposure, these values decrease by approximately 1 eV [7,9]. However, as shown in recent studies, these values remain high enough to allow MoO<sub>3</sub> to stay an efficient ABL if the highest occupied molecular orbital (HOMO) of the organic material is less than 5.9-6 eV, which is often the case in the typical electron donor materials [7]. It has also been shown that oxygen deficiency promotes hole transfer through the creation of band gap states.

Due to the high values of the IP energy of  $MoO_3$ , any hole transport via the valence band is prohibited, while the energy alignment between the band conduction minimum, BC, of  $MoO_3$  and the HOMO of the organic material is favorable for electron transfer between the two materials. That means that hole injection into the organic film proceeds via an electron transfer from the HOMO of the organic material to the band conduction of  $MoO_3$  in the case of organic light emitting diodes, whereas in the case of OPVCs, the photogenerated hole recombines with an electron at the interface between  $MoO_3$  and the organic layer, indicating that  $MoO_3$  works as a charge recombination layer. From this discussion,  $MoO_3$  cannot be an electron blocker because its conduction edge, CB, is too low. Therefore, the proposition of using  $MoO_x$  as a CBL is not an incongruous idea, especially because  $MoO_x$  tends to be metallic. Moreover, Vasilopoulou *et al.* [10] showed that the electron injection in an OLED based on poly[(9,9-di-n-octylfluorenyl-2,7-diyl)-alt-(benzo[2,1,3]thiadiazol-4,8-diyl)] (F8BT) can be significantly improved by inserting a very thin layer (5 nm) of partially reduced molybdenum oxide ( $MoO_{2.7}$ ) between the aluminum cathode and the organic emitting layer. Actually, after measuring the valence band maximum energy of  $MoO_x$  by UPS to be equal to 7.1 eV and the band gap of  $MoO_3$  to be 3 eV, they conclude that the conduction band minimum is at approximately 4.1 eV,

which is in good agreement with the work function of Al (4.3 eV). This energy alignment results in a relatively low electron injection barrier height. In addition, the states present in the band gap of  $MoO_x$  may increase both the electron injection from Al and the conductivity of the oxide layer. More recently, Jin *et al.* [11] showed that the efficiency of OPVCs can be improved through the use of bathophenanthroline/molybdenum oxide (Bphen/MoO<sub>x</sub>) as a compound cathode buffer layer. OPV cells based on planar  $CuPc/C_{60}$  diodes were used in this work. It was shown that optimum performances are achieved when the thickness of layers constituting the Bphen/MoO<sub>x</sub> CBL is 2 nm/5 nm, respectively. They attributed this improving effect to the fact that the presence of Bphen prevents the formation of a diode at the contact  $MoO_3/C_{60}$ , while  $MoO_3$  prevents damage to Bphen during Al deposition. To justify good band matching among Al (Wf = 4.3 eV),  $MoO_3$  (Wf = 5.3–6.2 eV depending on the experimental conditions) and  $C_{60}$  (lowest unoccupied molecular orbital (LUMO) 3.7 eV), Jin *et al.* proposed a dipole value of 3 eV at the interface of MoOx/Bphen, using a value issued from the bibliography.

As a matter of fact, the work function of MoO<sub>3</sub> is not the only important parameter at such complex interfaces; the Alq<sub>3</sub>/MoO<sub>3</sub> interface is also crucial. In the case of conventional CBL, Alq<sub>3</sub> protects C<sub>60</sub> from damage incurred during aluminum deposition onto the organic material. Earlier studies show that there is actually some cathode metal diffusion into the organic under layer [12]. However, if the CBL should be thick enough to protect the electron accepting layer, it should also not block all charge carriers. The HOMO and LUMO values of Alq<sub>3</sub> are 5.9 and 3 eV, respectively. Because the LUMO value of the fullerene is 4.4 eV, the offset energy between the LUMO of the fullerene and that of the Alq<sub>3</sub> is large, and the electrons must overcome a large energy barrier to reach the Al cathode in the case of electron transport via LUMO levels. To circumvent this difficulty, it has been proposed [13] that the charge transport in the CBL is due to damage induced during deposition of the cathode, which introduces conducting levels below its LUMO and explains why the transport of electrons is not impeded. Therefore, in the case of a double CBL, the relative thickness of both layers will either allow or disallow the presence of these gap states in Alq<sub>3</sub>. Furthermore, the position of these energy levels relative to the Fermi level of MoO<sub>3</sub> will be decisive as regards the passage of electrons.

Thus, because we used nearly similar structures in our laboratory, *i.e.*, planar heterojunctions based on the CuPc/C<sub>60</sub> junction [14], in the present paper, we probed OPVCs using tris-(8-hydroxyquinoline) aluminum (Alq<sub>3</sub>) as the EBL, leading to an Alq<sub>3</sub>/MoO<sub>3</sub> compound CBL. Even if our results are not identical to those mentioned above, they converge on those of Jin *et al.* [11], based on the time of exposure in air. These results are discussed in terms of the variation in the MoO<sub>3</sub> work function due to air contamination. Moreover, we show that the lifetime of the OPVCs with MoO<sub>3</sub> in their CBL is significantly improved.

# 2. Experimental

The OPVCs used were  $ITO/MoO_3/CuPc/C_{60}/Alq_3/MoO_3/Al/a$ -Se with different thicknesses constituting the  $Alq_3/MoO_3$  couple. The different films were deposited in thin film form by sublimation under vacuum ( $10^{-4}$  Pa), without breaking the vacuum.

The standard substrate dimensions were 25 mm by 25 mm. Because ITO covered the entire glass substrate, some ITO must be removed to obtain the under electrode. After masking a broad band of

25 mm by 20 mm, the ITO was etched using Zn + HCl as the etchant [14]. Before thin film deposition, the ITO coated glass substrate was scrubbed with soap, rinsed with distilled water, dried and then placed in the vacuum chamber.

To test the effect of  $MoO_3$  on the performance of the OPVCs when introduced into the CBL, we used the classical planar heterojunction structure  $CuPc/C_{60}$ ; the ABL was, as discussed above, a thin  $MoO_3$  film, and the cathode was an aluminum film. The CBL was a double layer of aluminum tris(8-hydroxyquinoline) (Alq<sub>3</sub>) [14] and  $MoO_3$ .

Without a protecting layer, the instability of solar cells in ambient air causes rapid deterioration in all performance, and non-encapsulated devices are practically dead after approximately 8 h in air. To mitigate this instability, prior to breaking the vacuum, an encapsulating layer of amorphous selenium (a-Se) approximately 40 nm in thickness was thermally evaporated. The selenium protective coating layer has been proven to be efficient in protecting the under layers from oxygen and water vapor contamination, at least during the early hours of ambient air exposure [14]. This encapsulation hinders, but does not eliminate, the oxygen and water vapor diffusion processes. Therefore, the protective layer, which increases the lifetime of solar cells and prolongs the duration of the process, thus improves the precision of this study on the effect of an EBL on this process.

The thickness of the thin films and deposition rates were estimated *in situ* using a quartz monitor. We used a 3 nm thick  $MoO_3$  layer as the ABL because, as discussed above,  $MoO_3$  is well known as a very efficient ABL in optoelectronic organic devices. According to a previous study [14], the thickness of the CuPc layer was 35 nm, and that of the  $C_{60}$  layer was 40 nm.

The relative thickness of the constituents of the Alq<sub>3</sub>/MoO<sub>3</sub> CBL was used as a parameter. The cathode was an aluminum film 100 nm thick, deposited by evaporation. The effective area of each cell was 0.16 cm<sup>2</sup>.

The main focus of this work was to study the influence of the value of the MoO<sub>3</sub> work function, when used as the CBL, on the OPV cell performance, *i.e.*, on the band matching at the interface cathode/EA. We varied the thickness of the Alq<sub>3</sub>/MoO<sub>3</sub> couple from 9 nm/0 nm to 2 nm/7 nm, with intermediary values of 6 nm/3 nm and 3 nm/6 nm. The lifetime of the OPVCs was studied through the protocol proposed in ref [15]. Following this protocol, the procedure used to study the aging process of our OPV cells corresponds to the intermediate level labeled "Level 2" The operational lifetimes have been measured under AM1.5, in air and at room temperature. The experimental conditions during the experiment were quite stable, *i.e.*, the temperature was maintained at  $T = 20 \pm 2$  °C and the humidity at 60%  $\pm$ 5%. Between each measurement, samples were stored in air and in the light of day, without artificial light. Cells were maintained in open circuit conditions. It should be noted that at least nine diodes are used in a cycle of deposit and that three cycles of deposits were used for the aging study.

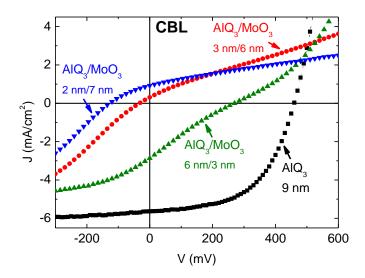
The work functions of different CBLs have been measured using a Kelvin probe instrument (KPTechnology Model SKP5050). The vibrating probe consists of a stainless steel tip 10 mm in diameter having a work function of 4.947 eV. For the measurements, the tip is calibrated against a gold surface. This calibration value varied by approximately 20–30 meV before and after each measurement, thus keeping the measurement error at 30 meV. The non-scanning mode is used to measure the work function with approximately 500 repetitions for a single point. The work function of the sample is obtained by adding the measured work function (WF) to the correction factor (4.947 eV). The Kelvin method measures the contact potential difference (CPD) between the tip and the surface of

the sample that are brought into contact as a result of Fermi energy equalization. The vibrating capacitor consists of the surface of the sample being tested, the reference surface of the electrode and the insulating medium between them. The CPD is evaluated by inducing an AC current flow and by the vibration of one of the surfaces with respect to the other in the vibrating capacitor. The contact potential difference is then measured by determining the compensating voltage required to null this current. The resolution of the measurements is 3 meV.

#### 3. Results and Discussion

The measurements made just after the realization of cells show that the presence of MoO<sub>3</sub> in the CBL systematically induces degradation of the OPV cell performance, which worsens with increasing thickness of the MoO<sub>3</sub> layer (Figure 1). However, when MoO<sub>3</sub> is present in the CBL, there is a continuous, systematic improvement in the OPVC efficiency during the first 5–6 days of room air exposure, whereas its efficiency decreases continuously when the CBL contains only Alq<sub>3</sub> (Figures 2–4).

**Figure 1.** J-V characteristics of ITO (100 nm)/MoO<sub>3</sub> (3 nm)/CuPc (35 nm)/C<sub>60</sub> (40 nm)/Alq<sub>3</sub> (x nm)/MoO<sub>3</sub> (y nm)/Al organic photovoltaic cells (OPVCs) with different thicknesses for the constituents of the Alq<sub>3</sub>/MoO<sub>3</sub> couple.



In fact, just after realization, when MoO<sub>3</sub> is 3 nm thick (Figure 1), the J-V characteristics are S-shaped. This effect increases dramatically with MoO<sub>3</sub> thickness (Figure 1) because when the MoO<sub>3</sub> thickness is 6 nm, the sign of the photocurrent is inverted, and this effect is accentuated for 7 nm thick MoO<sub>3</sub>.

Nevertheless, after air exposure, there is progressive improvement of the OPVC performance during the first few days, regardless of the thickness of the MoO<sub>3</sub> layer in the CBL.

This improvement is spectacular in the case of the CBL with a MoO<sub>3</sub> film thickness of 6 nm because there is an inversion in the direction of the rectifying effect (Figures 2 and 3).

**Figure 2.** Evolution of the J-V characteristics over the duration of room air exposure of an OPVC with Alq<sub>3</sub> (3 nm)/MoO<sub>3</sub> (6 nm) as the cathode buffer layer (CBL).

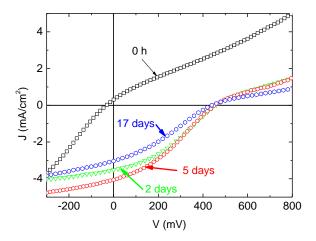


**Figure 3.** Variation with time of the typical performance of an OPVC with Alq<sub>3</sub> (3 nm)/MoO<sub>3</sub> (6 nm) as the CBL: ( $\blacksquare$ ) Jsc, ( $\bullet$ ) Voc, ( $\triangle$ ) FF and ( $\blacktriangledown$ )  $\eta/2$ .

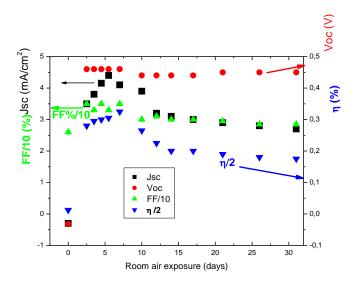
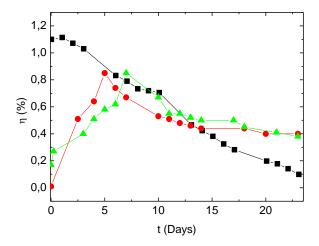


**Figure 4.** Variation with time of the efficiency of OPVCs with different CBLs: ( $\blacksquare$ ) CBL = Alq<sub>3</sub> (9 nm); ( $\bullet$ ) CBL = Alq<sub>3</sub> (6 nm)/MoO<sub>3</sub> (3 nm); ( $\blacktriangle$ ) CBL = Alq<sub>3</sub> (3 nm)/MoO<sub>3</sub> (6 nm).

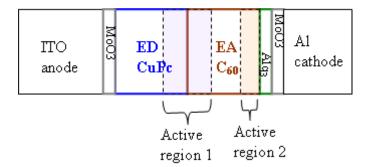


Therefore, ultimately, if we compare the performances of the different OPVCs after approximately 6 days of air exposure, the OPVCs with MoO<sub>3</sub> in their CBL exhibit similar efficiencies as those without MoO<sub>3</sub>, as can be seen in Figure 4. Moreover, the efficiency of the OPVCs with MoO<sub>3</sub> in their CBL becomes higher than that obtained with the classical Alq<sub>3</sub> CBL after 11–12 days of air exposure.

In Figure 3, we show the typical evolution of the different OPVC parameters as a function of air exposure time for the OPVCs using "Alq<sub>3</sub> (3 nm)/MoO<sub>3</sub> (6 nm)" as the CBL. The sign of the photocurrent has a striking effect. Immediately after device preparation, there is a positive photocurrent in the second quadrant, but its value is very small (Figures 1 and 2). After aging, the sign of the photocurrent becomes negative, as expected (Figure 2). The absolute values of Jsc and the OPVC efficiency  $\eta$  increase gradually over the first 5–6 days of air exposure. Then, there is a progressive decrease in Jsc and  $\eta$ . After 15 days,  $\eta$  reduces to approximately half its maximum value, which is attributed to degradation of the device from C<sub>60</sub> contamination [16]. The device then stabilizes for a long time (t > 4 months) at a value that is slightly less than half of the initial yield.

Regardless of the MoO<sub>3</sub> thickness in the CBL and the duration of aging, the J-V characteristics are S-shaped, except when they reach their maximum performance level. It is known that S-shaped J-V characteristics are typical for the formation of a reverse diode at the contact electrode/organic material [17,18]. This effect means that in the present structures, band bending occurs not only at the  $CuPc/C_{60}$  interface but also at the  $C_{60}$ /cathode interface (Figure 5).

**Figure 5.** Schematic representation of an OPVC with localization of the active regions.



These S-shaped J-V characteristics indicate the formation of a barrier at the  $C_{60}$ /cathode interface. In the case of the J-V characteristics of Figure 1, the band bending near the  $C_{60}$ /cathode interface must be larger than that at the  $CuPc/C_{60}$  interface, resulting in an opposite sign of the short circuit current. The formation of a barrier at the  $C_{60}$ /cathode interface is due to the presence of  $MoO_3$  in the CBL because there are no S-shaped characteristics when the CBL is only a film of  $Alq_3$  (Figure 1). The formation of this barrier can be explained by the very high work function of  $MoO_3$ . Actually, it is now well accepted that after deposition under vacuum by sublimation, the work function of  $MoO_3$  is approximately 6.2 eV [7]. With this high Wf value, the band structure of the interface is such that at the  $C_{60}/Alq_3/MoO_3/Al$  interface, the passage of holes is easier than that of electrons (Figure 6a). This result explains the reversal of the structure when the thickness of the  $MoO_3$  layer (6 nm) is such that the probability of charge carriers crossing by the tunnel effect is very low. However, it was also shown that air exposure of  $MoO_3$  induces a Wf decrease of approximately 1 eV [9].

**Figure 6.** Band scheme of the  $C_{60}/Alq_3/MoO_3/Al$  interface (**a**) just after deposition and (**b**) after five days of air exposure.

In our case, using a Kelvin probe, we found that the work function of our MoO<sub>3</sub> thin films is 5.1–5.2 eV after air exposure, regardless of the CBL, whereas it is 5.6 and 5.9 eV for a fresh CBL containing Alq<sub>3</sub> (6 nm)/MoO<sub>3</sub> (3 nm) and Alq<sub>3</sub> (3 nm)/MoO<sub>3</sub> (6 nm), respectively. This result means that the band alignment at the interface Allq<sub>3</sub>/MoO<sub>3</sub> depends on the relative thickness of these layers. Nevertheless, just after deposition, regardless of the value of the MoO<sub>3</sub> work function, the work function remains sufficiently high to induce the formation of a barrier at the C<sub>60</sub>/cathode interface.

If, in the present study, the OPVCs were covered with a Se film, it would not prevent progressive air contamination. Furthermore, we have already shown that even if the amorphous selenium film used as an encapsulation layer stabilizes the OPVCs, it only delays oxygen/water contamination of the cells. Therefore, the evolution of the J-V characteristics of the OPVCs for the duration of air exposure corresponds to the progressive air contamination of the OPVCs. The first layer encountered by the diffused contaminant after crossing the Al polycrystalline film is the MoO<sub>3</sub> layer. Therefore, due to this progressive contamination, the Wf of MoO<sub>3</sub> will decrease gradually until it reaches its minimal value of 5.1 eV. In parallel, the height of the barrier present at the C<sub>60</sub>/cathode interface decreases, which justifies the progressive improvement in the efficiency of the OPVCs over the first 6 days of air exposure (Figure 6b).

For a longer exposure time, the contamination reaches the C<sub>60</sub> layer, and the performance of the OPVCs decreases. In fact, the oxygen/water contamination of C<sub>60</sub> increases its resistivity [16]. However, this contamination is significantly limited by the presence of MoO<sub>3</sub> in the ABL because the efficiency of the OPVCs with a classical CBL tends regularly towards 0, whereas that of OPVCs with MoO<sub>3</sub> in their CBL tends to stabilize at a value of nearly half their initial efficiency (Figure 4). The greater stability of the OPVCs with an Alq<sub>3</sub>/MoO<sub>3</sub> bilayer as the CBL can be attributed to the fact that MoO<sub>3</sub> deposited by the Joule effect under vacuum is oxygen deficient and tends to trap oxygen, thus preventing the lower organic layer from a high degree of contamination.

The difference between our results and those of reference 6 may be attributed to the facility of the Wf in varying with the history of the  $MoO_3$  layer. Indeed, the films deposited by Vasilopoulou *et al.* [10] are strongly oxygen deficient, which ensures that the Wf of their  $MoO_3$  is small.

#### 4. Conclusions

The presence and height of a barrier at the C<sub>60</sub>/Alq<sub>3</sub>/MoO<sub>3</sub>/Al interface strongly depends on the Wf function of the MoO<sub>3</sub> layer. This value depends on the composition and degree of contamination of the MoO<sub>3</sub> layer. In the case of an uncontaminated layer, the Wf is so high that the OPVCs are inverted. When the MoO<sub>3</sub> layer is sufficiently oxygen deficient and/or oxygen/air contaminated, its Wf decreases significantly to provide OPVCs with acceptable performance levels. Moreover, except for the first few days, the efficiency of the OPVC with a classical EBL is lower than that with MoO<sub>3</sub> in their CBL. This result means that, although the initial performance of the OPVCs without MoO<sub>3</sub> in their CBL is greater than that of OPVCs with MoO<sub>3</sub>, the OPVCs with MoO<sub>3</sub> in their CBL become the most promising later on, as their performance quickly exceeds that of the former and tends to remain stable over time.

## **Author Contributions**

The three authors, Linda Cattin, Mustapha Morsli, and Jean Christian Bernède, contributed equally to the cell realization experiments, characterization and interpretation of the results.

#### **Conflicts of Interest**

The authors declare no conflict of interest.

### References

- 1. Darling, S.B.; You, F. The case for organic photovoltaics. RSC Adv. 2013, 3, 17633–17648.
- 2. Kumar, P.; Chand, S. Recent progress and future aspects of organic solar cells. *Prog. Photovolt.* **2012**, *20*, 377–415.
- 3. Nikiforov, M.P.; Strzalka, J.; Jiang, Z.; Darling, S.B. Lanthanides: New metallic cathode materials for organic photovoltaic cells. *Phys. Chem. Chem. Phys.* **2013**, *15*, 13052–13060.
- 4. Bundgaard, E.; Krebs, F.C. Low band gap polymers for organic photovoltaics. *Sol. Energy Mater. Sol. Cells* **2007**, *91*, 954–985.
- 5. Krebs, F.C. All solution roll-to-roll processed polymer solar cells free from indium-tin-oxide and vacuum coating steps. *Org. Electron.* **2009**, *10*, 761–768.
- 6. Nikiforov, M.P.; Strzalka, J.; Darling, S.B. Delineation of the effects of water and oxygen on the degradation of organic photovoltaic devices. *Sol. Energy Mater. Sol. Cells* **2013**, *110*, 36–42.
- 7. Meyer, J.; Hamwi, S.; Kröger, M.; Kowalsky, W.; Riedl, T.; Kahn, A. Transitionn metal oxides for organic electronics: Energetics, device physics and applications. *Adv. Mater.* **2012**, *24*, 5408–5427.
- 8. Tseng, Y.-C.; Mane, A.U.; Elam, J.W.; Darling, S.B. Ultrathin molybdenum oxide anode buffer layer for organic photovoltaic cells formed using atomic layer deposition. *Sol. Energy Mater. Sol. Cells* **2012**, *99*, 235–239.
- 9. Irfan, I.; Ding, H.; Gao, Y.; Small, C.; Kim, D.Y.; Subbiah, J.; So, F. Energy level evolution of air and oxygen exposed molybdenum trioxide films. *Appl. Phys. Lett.* **2010**, *96*, 243307.

10. Vasilopoulou, M.; Palilis, L.C.; Georgiadou, D.G.; Argitis, P.; Kennou, S.; Sygeliou, L.; Kostis, I.; Papadimitropoulos, G.; Konofaos, N.; Liadis, A.A.; *et al.* Reduced molybdenum oxide as an efficient electron injection layer in polymer light-emitting diodes. *Appl. Phys. Lett.* **2011**, *98*, 123301.

- 11. Jin, F.; Chu, B.; Li, W.; Su, Z.; Zhao, B.; Yan, X.; Zhang, F.; Fan, D.; Zhang, T.; Gao, Y.; *et al.* Improvment in power conversion efficiency and long-term lifetime of organic photovoltaic cells by using bathophenanthroline/molybdenum oxide as compound cathode buffer layer. *Sol. Energy Mater. Sol. Cells* **2013**, *117*, 189–193.
- 12. Yapi, A.S.; Toumi, L.; Lare, Y.; Soto, G.M.; Cattin, L.; Toubal, K.; Djafri, A.; Morsli, M.; Khelil, A.; del Valle, M.A.; *et al.* On the influence of the exciton-blocking layer on the organic multilayer cells properties. *Eur. Phys. J. Appl. Phys.* **2010**, *50*, 30403:1–30403:8.
- 13. Rand, B.B.P.; Li, J.; Xue, J.; Holmes, R.J.; Thompson, M.E.; Forrest, S.R. Organic Double-Heterostructure Photovoltaic Cells Employing Thick Tris(acetylacetonato)ruthenium(III) Exciton-Blocking Layers. *Adv. Mater.* **2005**, *17*, 2714–2718.
- 14. Berredjem, Y.; Karst, N.; Boulmokh, A.; Gheid, A.H.; Drici, A.; Bernède, J.C. Optimisation of the interface "organic material/aluminium" of CuPc/C<sub>60</sub>based photovoltaic cell. *Eur. Phys. J.* **2007**, *40*, 163–167.
- 15. Gevorgyan, S.A.; Medford, A.J.; Bundgaard, E.; Sapkota, S.B.; Schleiermacher, H.-F.; Zimmermann, B.; Würfel, U.; Chafiq, A.; Lira-Cantu, M.; Swonke, T.; *et al.* An inter-laboratory stability study of roll-to-roll coated flexible polymer solar modules. *Sol. Energy Mater. Sol. Cells* **2011**, *95*, 1398–1415.
- 16. Hamed, A.; Sun, Y.Y.; Tao, Y.K.; Meng, R.L.; Hor, P.H. Effects of oxygen and illumination on the *in situ* conductivity of C60 thin films. *Phys. Rev. B* **1993**, *47*, 10873–10880.
- 17. Kouskoussa, B.; Morsli, M.; Benchouk, K.; Louarn, G.; Cattin, L.; Khelil, A.; Bernède, J.C. On the improvement of the anode/organic material interface in organic solar cells by the presence of an ultra-thin gold layer. *Phys. Status Solidi A* **2009**, *206*, 311–315.
- 18. Lare, Y.; Kouskoussa, B.; Benchouk, K.; OuroDjobo, S.; Cattin, L.; Morsli, M.; Diaz, F.R.; Gacitua, M.; Abachi, T.; del Valle, M.A.; *et al.* Influence of the exciton blocking layer on the stability of layered organic solar cells. *J. Phys. Chem. Solids* **2011**, 72, 97–103.
- © 2014 by the authors; licensee MDPI, Basel, Switzerland. This article is an open access article distributed under the terms and conditions of the Creative Commons Attribution license (http://creativecommons.org/licenses/by/3.0/).